Why are plants green? An investigation into the mathematical details of the paper `Cost and color of photosynthesis'

Verburg, D.

D. Verburg

Why are plants green?

An investigation into the mathematical details of the paper
'Cost and color of photosynthesis'

Bachelor thesis, May 20th, 2011

Supervisor: Dr. S.C. Hille

Mathematisch Instituut, Universiteit Leiden

Preface

In January 2010 Marcell A. Marosvölgyi and Hans J. van Gorkom published an article named *Cost and color of photosynthesis* [1]. In this article an equation is derived that gives the optimal energy production through photosynthesis relative to the cost in maintaining the 'light harvesting' system. In this bachelor thesis we set out to understand the model assumptions and the equations which follow from the model derived in [1]. We also wanted to see if the method of 'map iteration' worked for finding solutions to the equations obtained. That is, firstly to investigate whether these iterations would converge to a solution for each starting point and secondly if the obtained solution is unique. Since this was not possible by hand MATLAB was used for simulation and iteration.

Due to the limited amount of time available for this bachelor project we were not able to solve all the questions we came up with. A lot of time was used in understanding the main article because of its interdisciplinary character; covering biology, biochemistry, physics and of course mathematics. Unfortunately we could not exchange views with the authors to verify our ideas, clarify possible misunderstandings from our side or possible errors from their in the article. We hope that this will be done in near future, after the completion of this bachelor project and the writing of this thesis.

Daniëlle Verburg

Contents

1 Introduction

This thesis is on the mathematics related to the question stated in the title: 'Why are plants green?'. Plants are green because the pigments, which play a role in the photosynthesis process, especially chlorophyll, do not absorb the green part of the light spectrum. So actually the question is why this is the case. There are several ways to approach this question, e.g. looking at the pigment's chemical structure. Interestingly in [1] the answer is sought using an evolutionary perspective, connected to a 'power budget-reasoning'. In order to provide some background for the way this problem was addressed in [1] and the mathematical issues resulting from that paper, which are the subject of this thesis, we begin with some explanation of the relevant biological and biophysical processes in plants.

1.1 Biological background

Plants get most of their energy from the biochemical process photosynthesis. The plant uses the light energy from the sun in the photosystem to produce chemically stored energy, e.g. in the form of sugar (glucose). The absorption of energy is taking place in the photosystem as a result of the products from the light reactions. These reactions use the sunlight and water to form chemicals which are used in the dark reactions (Calvin cycle) to produce glucose which will be stored for later use, e.g. in the form of starch.
The goal of this thesis is to study the system of nonlinear equations that results from the problem of optimizing the energy that can be used for growth, reproduction and defence. The assumption is made, that plants with optimal functioning photosystem have evolutionary advantage over those that do not. The process of evolution has resulted in plants with such an optimal system. So one would expect the solution to the optimisation problem to be observable in nature.

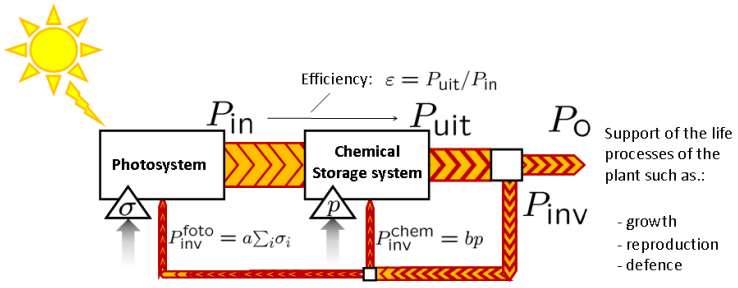

Figure 1: Energy flows in the photosynthesis system

Figure 1 show a model for the energy flows in the photosystem. P_{in} is the maximal power the photosystem can produce from sunlight on theoretical grounds, given the parameter setting σ (to be explained below in further detail). The chemical storage system, with

parameter p, is able to turn a fraction ϵ (*efficiency*) into chemically stored energy. Of course energy is needed for the support of the photosystem and for the chemical storage. The required power needed to invest in maintenance of the photosynthesis system is P_{inv}. It is split into two parts: one for maintenance of the photosystem, $P_{\text{inv}}^{\text{foto}}$, and the other for the chemical storage system, $P_{\text{inv}}^{\text{chem}}$. P_O is the net power available for other processes in the plants: $P_O = P_{\text{uit}} - P_{\text{inv}}$. A more detailed explanation can be found below.

1.2 Mathematical modelling approach

As mentioned in the biological background the plant uses sunlight for energy. The first step in the approach in [1] is, that the continuous light frequency spectrum is discretized. That is, the light frequency spectrum will be divided in small *frequency* bands, ranging from ν_0 until ν_n. We put $\Delta\nu_i := \nu_{i+1} - \nu_i$, $(i = 0, 1, \ldots, n-1)$. These steps will not be all equal. There will be no need to look at frequencies $\nu < \nu_0$ and $\nu > \nu_n$ since those are too low, respectively high frequency for photopigments to be absorbed for biochemical reasons.

Beer-Lambert's Law ($I(x) = I_0 e^{-\alpha x}$) applies to the absorption of light energy, in this case sunlight. In this law I_0 is the intensity of the light at the surface of a particular absorbing material, α is the absorption coefficient and $I(x)$ is the intensity at penetration depth x into the substance, in our case leaf tissue. The coefficient α depends on frequency in general. For this thesis we will look at the most effective α_i for every frequency interval $\nu_i \leq \nu \leq \nu_{i+1}$. The product $\sigma_i := \alpha_i x$ will be the so-called *absorption cross-section*. Notice that the fraction of the incoming sunlight energy in the frequency band $\nu_i \leq \nu \leq \nu_{i+1}$ that will be absorbed is $1 - e^{-\sigma_i}$. The goal of this thesis is to find a distribution for the σ_i such that the net power available to the plant's biological processes, P_O, is optimal.

Now some equations will be introduced and together they will give the master equation which will be used for the optimisation of P_O. The reader may consult [1] or [2] for further details of the derivation. The total number of absorbed photons per time per unit area, the *excitation frequency* for the frequency band from ν_0 to ν_n will be given by

$$J_L = \sum_{i=0}^{n-1} I_{0,i} \cdot (1 - e^{-\sigma_i}), \tag{1}$$

where $I_{0,i}$ denotes the number of incoming photons per unit time per unit area onto the leaf surface from sunlight in the frequency band $[\nu_i, \nu_{i+1}]$. In absence of sunlight, there is still some energy for the plant to absorb caused by thermal radiation. We assume an ideal situation: that of black-body radiation from the surroundings. The resulting photon flux in the frequency band $[\nu_i, \nu_{i+1}]$ is denoted by $I_{BB,i}$, in which BB stands for black-body radiation. It can be calculated by Planck's Law, (see forthcoming Section 3.2),

$$I(\nu, T) = h\nu \cdot \frac{2\nu^2}{c^2} \cdot \frac{1}{e^{h\nu/kT} - 1}. \tag{2}$$

The excitation in darkness due to black-body radiation then equals

$$J_D = \sum_{i=0}^{n-1} \sigma_i \cdot I_{BB,i}, \tag{3}$$

according to [1], [4]. J_L and J_D are called excitation frequency respectively for the light and the darkness. Looking at these excitation frequencies in relation to each other we get

$$Q = \frac{J_L + J_D}{J_D} = 1 + \frac{J_L}{J_D} \approx \frac{J_L}{J_D} \tag{4}$$

The approximation is because J_L is much bigger than J_D, typically. According to [1], [4] the maximal power that can be produced from the light by this process is given by

$$P_{\text{in}} = J_L \cdot kT \cdot \ln Q \approx J_L \cdot kT \cdot \ln \frac{J_L}{J_D} \tag{5}$$

In (5) kT, the thermodynamic energy, is a constant, where T is the absolute temperature and k is the Boltzmann constant, namely $k \approx 8.617 \times 10^{-5}\text{eV} \cdot \text{K}^{-1}$. For this thesis $T = 295\text{K}$ (room temperature) will be used and so $kT = 0.0254$ eV $= 4.07 \times 10^{-21}$ J For simplicity we write

$$\mu := kT \cdot \ln \frac{J_L}{J_D}. \tag{6}$$

Part of the energy absorbed in the photosystem is converted into a form suitable for further use in the plant. The power that is finally produced during the photosynthesis process will be called

$$P_{\text{uit}} = \epsilon(p, P_{\text{in}}) P_{\text{in}}, \qquad 0 \leq \epsilon \leq 1, \tag{7}$$

where ϵ is the efficiency in the conversion of energy, from P_{in} to P_{uit}. p is a parameter. As shown in Figure 1 energy is needed to keep the photosystem and chemical storage going. In the model these are assumed to be given by

$$P_{\text{inv}}^{\text{foto}} = a \sum_{i=0}^{n} \sigma_i, \qquad P_{\text{inv}}^{\text{chem}} = bp. \tag{8}$$

Then

$$P_O = P_{\text{uit}} - P_{\text{inv}} = \epsilon(p, P_{\text{in}}) P_{\text{in}} - a \sum_i \sigma_i - bp. \tag{9}$$

In [1] one makes the particular choice

$$\epsilon(p, x) = \frac{p}{p + x}. \tag{10}$$

Thus, p is the level of P_{in} at which $\epsilon = \frac{1}{2}$. This completes the model.

1.3 The master equation

Given $a \geq 0$ and $b \geq 0$, and the particular choice for ϵ as in (10) one is looking for solutions for $\sigma = (\sigma_0, \sigma_1, \ldots, \sigma_n)$ and p such that P_O is optimal. In [1] one then imposes the critical point conditions

$$\frac{\partial P_O}{\partial \sigma_i} = 0, \qquad \frac{\partial P_O}{\partial p} = 0. \tag{11}$$

From these conditions, equation (9) and the particular form of ϵ as in (10), one obtains the condition

$$\frac{\partial P_{\text{in}}}{\partial \sigma_i} = \frac{a}{2(1-\sqrt{b})}. \tag{12}$$

Implicitly, we obtain the condition that $0 \leq b < 1$. Computing $\frac{\partial P_{\text{in}}}{\partial \sigma_i}$ from (5) now yields the system of equations, that is the starting point of this thesis:

$$I_{0,i} \cdot e^{-\sigma_i} = \frac{kT}{\mu(\sigma) + kT} \cdot \left[I_{BB,i} \cdot \frac{J_L(\sigma)}{J_D(\sigma)} + \frac{a}{kT \cdot 2(1-\sqrt{b})} \right]. \tag{13}$$

We want to solve for σ_i.

1.4 Comparison with the paper's master equation

We have derived (13) but this one is a little different from the master equation in [1] derived along similar lines. There the equation reads as follows:

$$I_{0,i} \cdot e^{-\sigma_i} = \frac{kT}{\mu + kT} \cdot \left[I_{BB,i} \cdot \frac{J_L}{J_D} + \frac{C_{P_{\text{in}}}}{C_{P_{\text{in}}} + C_G} \cdot \frac{J_L \cdot \mu}{h\nu_i (\sum_j \sigma_i / h\nu_j)} \right]. \tag{14}$$

We would like to make three remarks at this point.
First, the system of equations (14) for a critical point of P_O as derived in [1] differs from (13), as the last term within the brackets on the right is σ-dependent. It appears that this might be caused by a minor mistake, or 'hidden assumption' in the derivation of $\frac{dP_G}{dP_{\text{sat}}}$ in the Supplementary Material of [1], p4. Note however, that for vanishing cost of the photosystem, i.e. $C_{\text{Pin}} = 0$ in (14) or $a = 0$ in (13), the two master equations agree. In that case we would expect an infinitely large absorption cross-section σ_i for all i to be a solution: all light is harvested. In that case J_D, as expressed by (3), becomes infinitely large though, while J_L remain finite. Therefore the approximation made in (4) fail and so should the remainder of the derivation, hence master equations (13) and (14).

Second, having a critical point at some σ^* does not guarantee the existence of a maximal (or minimal) value for P_O at σ^*. Further conditions are required.
Third, the domain of P_O as a function of σ and p is not the open set $\mathbb{R}^{n+1} \times \mathbb{R}$, but the *closed cone* $\mathbb{R}_+^{n+1} \times \mathbb{R}_+$, where $\mathbb{R}_+ = [0, \infty)$. Thus we are looking for extreme values of P_O on a domain *with boundary*. This deserves particular attention, because of the possibility of extreme values lying on the boundary, where $\frac{\partial P_O}{\partial \sigma_i}$ need not all vanish.

1.5 Conditions for optimal net power

We can say that we are looking for the optimum of P_O with (σ, p) in $\Omega = \mathbb{R}_+^n \times \mathbb{R}_+$. We will see that for a $\sigma_i \in \Omega$ the derivation of condition (12) needs the condition that $\frac{\partial P_O}{\partial \sigma_i} = 0, i = 0, \ldots, n-1$ and $\frac{\partial P_O}{\partial p} = 0$. It is possible that σ_i lies on $\partial\Omega$. We may write Ω as a disjunct union of subsets $\Omega_\emptyset$ and $\partial\Omega_I$, where I is a (non-empty) subset of $\{0, 1, \ldots, n-1\} \cup \{*\}$ when we put

$$\partial\Omega_I = \{(\sigma_i, p) \in \Omega | \sigma_i = 0 \text{ if } i \in I \text{ and } p = 0 \text{ if } * \in I\} \tag{15}$$

Then P_O has a maximal value in $\partial\Omega_I$ if

$$\begin{cases} \frac{\partial P_O}{\partial \sigma_i} = 0 & \text{if } i \notin I, \\ \frac{\partial P_O}{\partial \sigma_i} < 0 & \text{if } i \in I. \end{cases} \tag{16}$$

and $\frac{\partial P_O}{\partial p} = 0$ if $* \in I$.

2 Finding solutions to the equation - abstract approach

We want to solve for σ_i in the system (13). We first observe, that (13) does not have any solution when some $I_{0,i} = 0$. In fact, $I_{BB,i} > 0$ and $\frac{J_L}{J_D} > 0$ for $\sigma \neq 0$. Therefore the part between brackets in the right hand side of (13) cannot become zero, nor can the factor in front.

So we must assume $I_{0,i} > 0$ for all i. Now we can divide by $I_{0,i}$ in (13) and obtain

$$e^{-\sigma_i} = \frac{1}{1 + \ln\left(\frac{J_L}{J_D}\right)} \cdot \left[\frac{I_{BB,i}}{I_{0,i}} \cdot \frac{J_L(\sigma)}{J_D(\sigma)} + \frac{a}{kT \cdot I_{0,i}} \cdot \frac{1}{2(1-\sqrt{b})}\right]. \tag{17}$$

We further rewrite (13) by defining $t_i := e^{-\sigma_i}$, which is the *transmission* of light for frequency ν_i. Since $\sigma_i \geq 0$, we have $0 < t_i \leq 1$. Thus $\sigma_i = -\ln t_i$. The master equation now becomes

$$t_i = \frac{1}{\ln\left(\frac{J_L}{J_D}\right) + 1} \cdot \left[\frac{I_{BB,i}}{I_{0,i}} \cdot \frac{J_L}{J_D} + \frac{a}{kT \cdot I_{0,i}} \cdot \frac{1}{2(1-\sqrt{b})}\right]. \tag{18}$$

Thus, if we define a map $F : (0,1]^n \to \mathbb{R}^n$ component-wise by the right hand side of (18), the problem we need to face is to determine all fixed points of F.

We approach the problem of finding fixed points of F by means of successive iteration which is also used in [1]. That is, we start with an initial value $t_0 \in (0,1]^n$ and define

$$t_n := F(t_{n-1}). \tag{19}$$

If $\lim_{n\to\infty} t_n =: t^*$ exists, and F is continuous at t^*, then t^* is a fixed point of F, because

$$F(t^*) = F(\lim_{n\to\infty} t_n) = \lim_{n\to\infty} F(t_n) = t^*. \tag{20}$$

In the middle step we need continuity of F at t^*. However, it is not clear from (18) that F maps $(0,1]^n$ into itself. We will first examine the iteration process numerically.

3 Simulation

We implemented the simulation of the iteration procedure in MATLAB (version 7.6.0 R2008a). See the Appendix for the code. In order to get interpretable t values, we modified F into $\tilde{F}$, such that $\tilde{F}_i(t) = 1$ when $F_i(t) > 1$ and $\tilde{F}_i(t) = 0$ when $F_i(t) < 0$.

3.1 Solar radiation data

Before we are able to start the simulation we need realistic values for the solar photon flux density distribution, $I_{0,i}$. We took $I_{0,i}$ from [3], which is provided by the American Society for Testing and Materials (ASTM). It was founded in 1898 with initial plans to find and solve problems in railtracks. Since 2005 there are more then 12,000 ASTM standards known. Some of these standards concern the sunlight spectrum, which are used for testing the performance of photovoltaic cells. Since 2005 ASTM is called ASTM International because the members are situated all over the world.

We used the sunlight irradiance distribution relative to wavelength (in nm) at a perpendicular incidence on the surface at sea level. See Figure 2, (right panel). It provides a sampling of $F_0(\lambda)$, which is the continuous distribution of solar irradiance (transmitted power per unit area per wavelength unit) at wavelengths λ_i ranging from 280 nm up to 4000 nm. The energy flux density associated to the *wavelength* in the range $[\lambda_i, \lambda_{i+1})$ equals

$$j_{E,i} = \int_{\lambda_i}^{\lambda_{i+1}} F_0(\lambda) d\lambda. \tag{21}$$

The corresponding photon flux density equals

$$I_{0,i} \approx \frac{j_{E,i}}{h\nu_i}. \tag{22}$$

Using an approximation for the integral in (21), we have

$$\begin{aligned} j_{E,i} &\approx \frac{1}{2}[F_0(\lambda_{i+1}) + F_0(\lambda_i)] \cdot \Delta\lambda_i & (23)\\ &\approx F_0(\lambda_i) \cdot \Delta\lambda_i, & (24) \end{aligned}$$

and we obtain[1]

$$I_{0,i} \approx \frac{F_0(\lambda_i)}{hc} \cdot \lambda_i \cdot \Delta\lambda_i \tag{25}$$

(in number of photons per m^2 per second). We have $\lambda = \frac{c}{\nu}$ in which ν is our chosen interval and $c = 299.8 \times 10^6$ m/s, the speed of light. $h = 4.136 \times 10^{-15}$ eV/s which is Planck's constant.

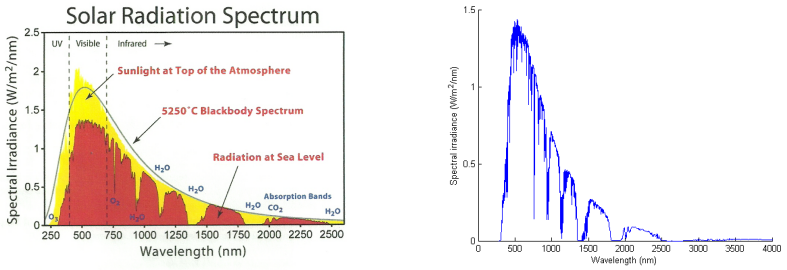

Figure 2: Solar Radiation Spectrum. Left: the energytransmission of the sun in wavelengths outside the atmosphere and on sealevel,[3]. Right: the energytransmission at sea level according to ASTM data used.

Figure 2 shows that the data used for $I_{0,i}$ is consistent with information found elsewhere, ([3]). Notice the gaps in the graphs around 1300 nm and around 1800 nm. These are caused by absorption of sunlight in the atmosphere by water vapour. In the data there are some zeros which will be a problem for (13) because we have to divide by $I_{0,i}$ (see remark in Section 2). This problem is solved since we only have to look at 400 nm - 700 nm since this is the visible light range, so effectively we will not have problems with the gaps.

3.2 Black-body photon flux distribution

A similar approach applies to the computation of $I_{BB,i}$. The photon flux density distribution relative to frequency in the interior of a black *box*, (see Figure 3), may be computed to be

$$F_{BB}(\nu) = 8\pi \cdot \left(\frac{\nu}{c}\right)^2 \cdot \frac{1}{e^{h\nu/kT} - 1} \tag{26}$$

(in number of photons per m^2 per second per unit frequency).[2] Then

[1] In the implementation we use the vector Iss for $(F_0(\lambda_i))_{i=0}^{n-1}$

[2] This expression has been derived from the formula for the spectral energy density per unit volume of therodynamic equilibrium cavity radiation as found on Wikipedia,('Planck's law'), for which we could not find an appropiate reference in the physics literature.

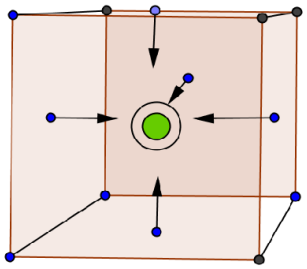

Figure 3: Black-body radiation from the 'walls' representing the environment.

$$
\begin{aligned}
I_{BB,i} &= \int_{\nu_i}^{\nu_{i+1}} F_{BB}(\nu)d\nu && (27)\\
&=^{*} -\int_{\lambda_i}^{\lambda_{i+1}} F_{BB}\left(\frac{c}{\lambda}\right)\cdot\frac{c}{\lambda^2}d\lambda && (28)\\
&= -8\pi c\cdot\int_{\lambda_i}^{\lambda_{i+1}} \frac{1}{\lambda^4}\cdot\frac{1}{e^{\frac{hc}{kT}\cdot\frac{1}{\lambda}}-1}d\lambda && (29)\\
&\approx 8\pi c\cdot\frac{1}{2}\left[\frac{1}{\lambda_i^4}\cdot\frac{1}{e^{\frac{hc}{kT}\cdot\frac{1}{\lambda_i}}-1}+\frac{1}{\lambda_{i+1}^4}\cdot\frac{1}{e^{\frac{hc}{kT}\cdot\frac{1}{\lambda_{i+1}}}-1}\right]\cdot\Delta\lambda_i && (30)\\
&\approx 8\pi c\cdot\frac{1}{\lambda_i^4}\cdot\frac{1}{e^{\frac{hc}{kT}\cdot\frac{1}{\lambda_i}}-1}\cdot\Delta\lambda_i && (31)\\
&\approx 8\pi c\cdot\frac{kT}{hc}\cdot\frac{1}{\lambda_i^3+\frac{1}{2}\cdot\frac{hc}{kT}\cdot\lambda_i^2}\cdot\Delta\lambda_i && (32)
\end{aligned}
$$

($^{*}\nu=\frac{c}{\lambda}, \lambda_i=\frac{c}{\nu_i}, d\nu=-\frac{c}{\lambda^2}d\lambda$). Notice that $\nu_{i+1}>\nu_i$ so $\lambda_{i+1}<\lambda_i$ and the minus sign in front of (29) is 'absorbed' into the integral by exchanging the bounds of the integral.

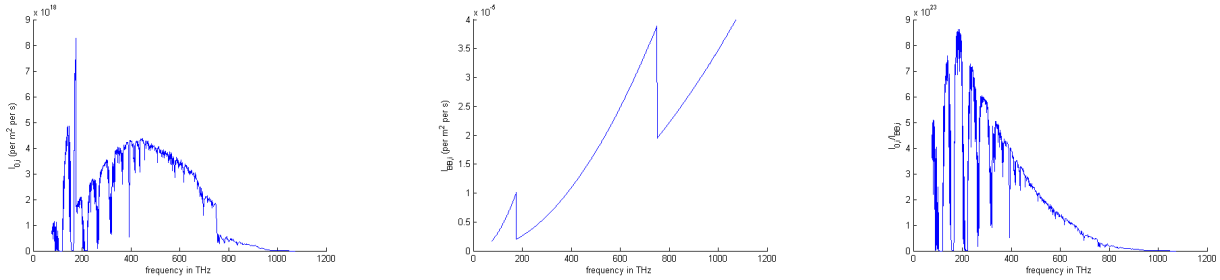

Figure 4: Left: $I_{0,i}$ vs ν_i, middle: $I_{BB,i}$ vs ν_i, right: $\frac{I_{0,i}}{I_{BB,i}}$ vs ν_i

In Figure 4 we plotted $I_{0,i}$ and $I_{BB,i}$ and $\frac{I_{0,i}}{I_{BB,i}}$ as function of ν_i. Notice in the left panel and middle panel that we have some 'jumps' in the graphs. These 'jumps' are the result of the choice made in the data from ASTM ([3]), since there the wavelength starts at 280 nm and goes up to 4000 nm, but not in equal steps. In the beginning there are steps of 0.5 nm, later it become 1.0 nm and in the end even 5.0 nm.

3.3 Simulation 1

We have simulated (17) for different a and b. Notice that we use the notation $\mathbf{1}$ for a vector with ones at each component (of the appropriate dimension. Notice that a (power required per unit cross-section per m^2 of leaf surface) has unit eV/m^2s. As said we have

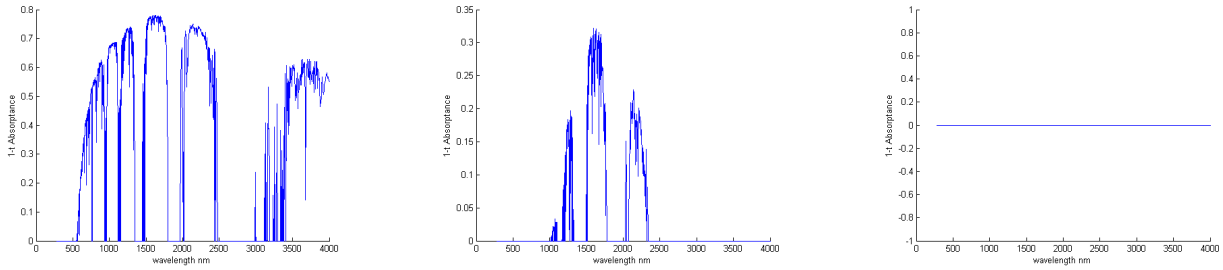

Figure 5: Simulation a=0.5, b=0.5, $t_0 = 0.9 \times \mathbf{1}$. Left is 1 iteration, the middle 4 iterations and the right 10 iterations

changed all the data from wavelength to frequency and by using (18) we have iterated F to obtain a possible solution. The results are not as expected. Figure 5 shows the iteration for $a = 0.5$, $b = 0.5$ and t_0 the initial vector $0.9 \times \mathbf{1}$. We see that after several iterations the graph is becoming smaller and after 10 iterations the graph has become a line at 0. So, looking at this in a biological sense it says that the plant should not absorb in order to become a 'strong' plant.
Of interest in Figure 6 and Figure 7 is the change of a and b. Between Figure 5 and Figure 6 we do not see a big difference in the first two graphs, since b has only changed from 0.5 to 0.01. The difference between Figure 6 and Figure 7 is not noticable which is strange because now we changed a from 0.5 to 0.

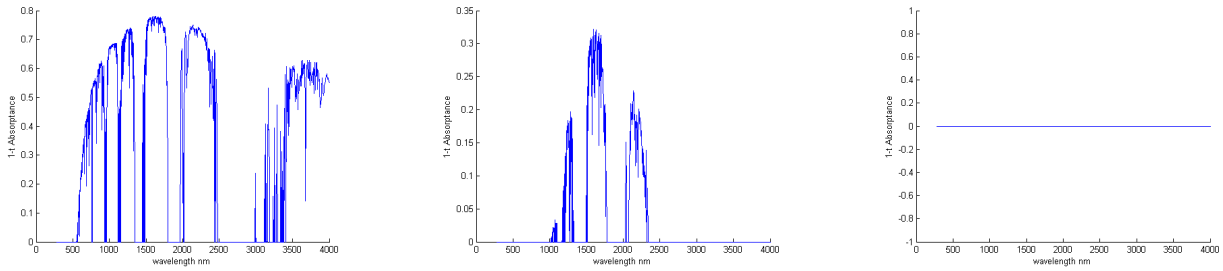

Figure 6: Simulation a=0.5, b=0.01, $t_0 = 0.9 \times \mathbf{1}$. Left is 1 iteration, the middle 4 iterations and the right 10 iterations

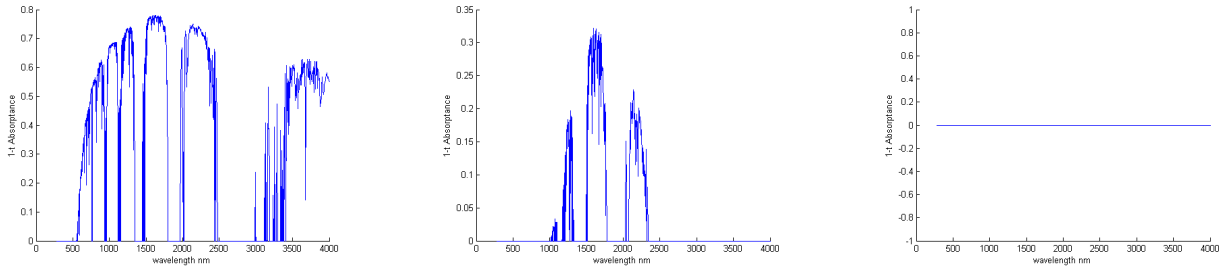

Figure 7: Simulation a=0, b=0.5, $t_0 = 0.9 \times \mathbf{1}$. Left is 1 iteration, the middle 4 iterations and the right 10 iterations

3.4 Discussion of simulation

Of course we have done several more simulations, also varying t_0 between 0 and 1 (results are not shown). Although the graphs are a little bit different the result is every time the same. After a small number of iterations we end up with the final graph of the three simulations shown here. It appears that something is completely 'wrong', since the final result makes no sense at all, in particular in the cost $a = 0$. The result we got for $a = 0$ was the one that raised most questions: looking at (17) you would not expect that the simulation goes to zero since only the second term between brackets becomes zero. Both in an approach, using (13) and the one from [1], which has the same master equation for $C_{\mathrm{P_{in}}} = 0$, the method of iteration converges to a result which is not a reasonable solution: biologically one would expect the system to harvest on all light frequencies when there is no cost. Thus we had the idea that the equation used in [1] must be wrong. This made us start to have another look at the equations and see what should be different.

4 A modified master equation

We go back to (1), this equation still holds. In our opinion (3) has to change to

$$J_D = \sum_{i=0}^{n-1} I_{BB,i} \cdot (1 - e^{-\sigma_i}), \tag{33}$$

because it is unclear why absorption of photons from black-body radiation should be treated different from those in sunlight. Also the approximation in (4) should not be made. We will continue with

$$Q = 1 + \frac{J_L}{J_D} \tag{34}$$

in the deriviation, instead of the approximation $Q \approx \frac{J_L}{J_D}$ made in (4). So (5) changes into

$$P_{\text{in}} = J_L \cdot kT \cdot \ln Q = J_L \cdot kT \cdot \ln\left(1 + \frac{J_L}{J_D}\right). \tag{35}$$

Again for simplicity we take $\mu := kT \cdot \ln\left(1 + \frac{J_L}{J_D}\right)$. Condition (12) will still hold in this case but (13) will not be the same. Our calculations to get a new equation for $e^{-\sigma_i}$ are as follows:

$$\begin{aligned}
\frac{\partial P_{\text{in}}}{\partial \sigma_i} &= \frac{\partial J_L}{\partial \sigma_i} \cdot \mu + J_L \cdot kT \cdot \frac{1}{1 + \frac{J_L}{J_D}} \cdot \frac{\partial}{\partial \sigma_i}\left(\frac{J_L}{J_D}\right) \\
&= \frac{\partial J_L}{\partial \sigma_i} \cdot \mu + J_L \cdot kT \cdot \frac{1}{1 + \frac{J_L}{J_D}} \cdot \frac{\frac{\partial J_L}{\partial \sigma_i} \cdot J_D - J_L \cdot \frac{\partial J_D}{\partial \sigma_i}}{J_D^2} \\
&= \frac{\partial J_L}{\partial \sigma_i}\left(\mu + J_L \cdot kT \cdot \frac{1}{J_D} \cdot \frac{1}{1 + \frac{J_L}{J_D}}\right) - \frac{J_L^2}{J_D^2} \cdot kT \cdot \frac{1}{\left(1 + \frac{J_L}{J_D}\right)} \cdot \frac{\partial J_D}{\partial \sigma_i} \\
&= \frac{\partial J_L}{\partial \sigma_i}\left(kT \cdot \ln\left(1 + \frac{J_L}{J_D}\right) + kT \cdot \frac{\frac{J_L}{J_D}}{1 + \frac{J_L}{J_D}}\right) - \frac{J_L^2}{J_D^2} \cdot kT \cdot \frac{1}{\left(1 + \frac{J_L}{J_D}\right)} \cdot \frac{\partial J_D}{\partial \sigma_i} \\
&= kT \cdot I_{0,i} e^{-\sigma_i}\left(\ln\left(1 + \frac{J_L}{J_D}\right) + \frac{\frac{J_L}{J_D}}{1 + \frac{J_L}{J_D}}\right) - I_{BB,i} \cdot e^{-\sigma_i} \cdot kT \cdot \frac{1}{1 + \frac{J_L}{J_D}} \cdot \frac{J_L^2}{J_D^2}.
\end{aligned}$$

This combined with (12) yields a new master equation:

$$e^{-\sigma_i} = \frac{a}{2(1 - \sqrt{b})kT} \cdot \frac{1}{I_{BB,i}} \cdot \left[\frac{I_{0,i}}{I_{BB,i}}\left(\ln\left(1 + \frac{J_L}{J_D}\right) + \frac{\frac{J_L}{J_D}}{1 + \frac{J_L}{J_D}}\right) - \frac{\frac{J_L^2}{J_D^2}}{1 + \frac{J_L}{J_D}}\right]^{-1}. \tag{36}$$

This equation looks more reasonable, because when $a = 0$ we get immediately that the iteration becomes 0 and so the absorptance $(1 - e^{-\sigma_i})$ becomes 1. This is what we expected

if you look at it from the biological point of view.

Let us put as before $t_i = e^{-\sigma_i}, i = 0, \ldots, n-1$. We may rewrite (36) as a fixed point equation $t = F(t)$. Notice that the right hand side of (36) actually is a function of $x = Q(t)$. Put $v_i = \frac{I_{0,i}}{I_{BB,i}}$. Then

$$v_i \left(\ln\left(1 + \frac{J_L}{J_D}\right) + \frac{\frac{J_L}{J_D}}{1 + \frac{J_L}{J_D}} \right) - \frac{\frac{J_L^2}{J_D^2}}{1 + \frac{J_L}{J_D}} = v_i(\ln x + 1 - \frac{1}{x}) - (x - 2 + \frac{1}{x}) \tag{37}$$

by noticing that

$$\frac{\frac{J_L^2}{J_D^2}}{1 + \frac{J_L}{J_D}} = \frac{\left(\frac{J_L^2}{J_D^2} - 1\right) + 1}{1 + \frac{J_L}{J_D}} = \left(\frac{J_L}{J_D} - 1\right) + \frac{1}{1 + \frac{J_L}{J_D}} = x - 2 + \frac{1}{x}. \tag{38}$$

(37) may be rewritten into

$$\begin{aligned} v_i(1 + \ln x) - \frac{v_i + 1}{x} - (x - 2) &= \frac{v_i x(1 + \ln x) - (x^2 - 2x + v_i + 1)}{x} \\ &= v_i(1 + \ln x) - \frac{[(x-1)^2 + v_i]}{x}. \end{aligned}$$

Thus, with $x = Q(t)$ and recalling that $v_i = \frac{I_{0,i}}{I_{BB,i}}$,

$$F_i(t) = G_i(x) = \frac{a}{2(1 - \sqrt{b}) \cdot kT} \cdot \frac{1}{I_{BB,i}} \cdot \frac{x}{v_i x(1 + \ln x) - v_i \left[1 + \frac{(x-1)^2}{v_i}\right]} \tag{39}$$

$$= \frac{a}{2(1 - \sqrt{b}) \cdot kT} \cdot \frac{1}{I_{0,i}} \cdot \frac{x}{x(1 + \ln x) - \left[1 + \frac{(x-1)^2}{v_i}\right]}, \tag{40}$$

provided $v_i \neq 0$ of course.

4.1 Properties of the iteration map

Now recall

$$Q(t) = 1 + \frac{\sum_i I_{0,i}(1 - t_i)}{\sum_i I_{BB,i}(1 - t_i)}. \tag{41}$$

Then it is clear that:

Lemma 1: *$t \mapsto Q(t)$ is continuous on $[0,1]^n \setminus \{\mathbf{1}\}$ and $Q(t) > 1$ for all $t \in [0,1]^n \setminus \{\mathbf{1}\}$.*

From (40) we see that $G_i(x)$ is discontinuous on $(1, \infty)$ only at points x at which $x(1 + \ln x) = 1 + \frac{1}{v_i}(x-1)^2$.

Lemma 2: *For each i there exists a unique $x_i^* > 1$, such that $x(1+\ln x) > 1 + \frac{1}{v_i}(x-1)^2$ for $1 < x < x_i^*$, $x(1+\ln x) < 1 + \frac{1}{v_i}(x-1)^2$ for $x > x_i^*$ and equality holds for $x = x_i^*$.*

Proof: Clearly, $x(1+\ln x) = 1 + \frac{1}{v_i}(x-1)^2$ for $x = 1$. The right hand side is a parabola with minimum at $x = 1$, while the left hand side is a convex function with tangent slope at $x = 1$ equal to 2, ($[x(\ln x + 1)]' = 2\ln x$). So there exists an interval $(1, \alpha)$, possible $\alpha = +\infty$ on which $x(1+\ln x) > 1 + \frac{1}{v_i}(x-1)^2$. Now consider the equation

$$x(1+\ln x) = 1 + \frac{1}{v_i}(x-1)^2 \tag{42}$$

on $(1, \infty)$. It is equivalent to

$$1 + \ln x = \frac{1 + \frac{1}{v_i}(x-1)^2}{x}. \tag{43}$$

Moreover,

$$h_i(x) := \frac{1 + \frac{1}{v_i}(x-1)^2}{x} = \frac{1}{v_i}x - \frac{2}{v_i} + \frac{1 + \frac{1}{v_i}}{x}. \tag{44}$$

That is, the right hand side in (43) has $\frac{1}{v_i}x - \frac{2}{v_i}$ as asymptote as $x \to \infty$. $x \mapsto 1 + \ln x$ intersects this asymptote at some point $x' > 1$.
At $x = 1$, the slope of $x \mapsto 1 + \ln x$ equals 1, while that of $x \mapsto \frac{1+\frac{1}{v_i}(x-1)^2}{x} = h_i(x)$ equals $\frac{1}{v_i} - \left(1 + \frac{1}{v_i}\right) = -1$. One has $h_i''(x) = 2 \cdot \frac{1+\frac{1}{v_i}}{x^3} > 0$ so the graph of h_i is convex. Moreover the minimum of h_i lies at $\sqrt{v_i^2 + 1}$ and the minimal value lies above the asymptote, so h_i lies above the asymptote on $(1, \infty)$. Since $x \mapsto 1 + \ln x$ is concave, there must exist $x_i^* > 1$ such that (43) holds for $x = x_i^*$. $\square$

Thus, we obtain

Proposition 1: *$F : [0,1]^n \backslash \{1\} \to \mathbb{R}$ is continuous except on the surfaces $Q(t) = x_i^*, i = 0, \ldots n-1$.*

Note that near $t = 1$, $Q(t)$ 'blows up', so for each i, $\{t \in [0,1]^n \backslash \{\mathbf{1}\} \,|Q(t) = x_i^*\} \neq \emptyset$. Moreover,

Proposition 2: *$F_i(t) > 0$ for $t \in [0,1]^n \backslash \{\mathbf{1}\}$ such that $Q(t) < x_i^*$.*

Proof: This follows directly from Lemma 2.

We would further like to remark that the set $Q(t) = x_i^*$ is a hyperplane:

$$Q(t) = x_i^* \quad \Leftrightarrow \quad \sum_j I_{0,j}(1-t_j) = x_i^* \sum_j I_{BB,j}(1-t_j) \tag{45}$$

$$\Leftrightarrow \quad \sum_j (I_{0,j} - x_i^* I_{BB,j}) t_j = \sum_j (I_{0,j} - x_i^* I_{BB,j}) \tag{46}$$

$$\Leftrightarrow \quad n_i \cdot t = c \tag{47}$$

for some vector $n_i \in \mathbb{R}^n$ and scalar c.

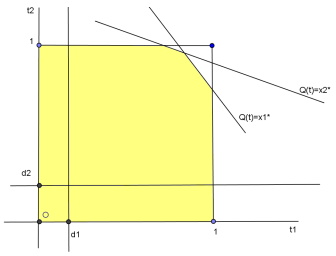

Figure 8: A possible configuration of the set of $Q(t) < x_i^*$

Note that

$$F_i(t) = G_i(x) = \frac{a}{2(1-\sqrt{b}) \cdot kT} \cdot \frac{1}{I_{0,i}} \cdot \frac{1}{(1+\ln x) - h_i(x)} \tag{48}$$

The previous discussion reveals that $G_i(x)$ can become arbitrarly large for $x \in (1, x_i^*)$. On the other hand the difference $(1+\ln x) - h_i(x)$ is bounded on $(1, x_i^*)$. Thus for each i thee exists $\delta_i > 0$ such that $F_i(t) \geq \delta_i$ for all $t \in [0,1]^n \backslash \{1\}$ for which $Q(t) < x_i^*$.

In Figure 8 a sketch is presented of a possible configuration of $t \in [0,1]^2 \backslash \{1\}$ for which $Q(t) < x_i^*$ for all i is yellow. Moreover we have indicated the location of δ_i. Unfortunately, we are not able (yet) to prove or disprove the existence of a subset C of

$$\bigcap_{i=0}^{n-1} \{t \in [0,1]^n \backslash \{1\} | Q(t) < x_i^*\} \tag{49}$$

that is mapped to itself by F. We continue our investigations by means of numerical simulations.

4.2 Simulation 2

The new master equation gives much more reasonable results. Figure 9 shows three simulations for different values of a and b. The first simulation shows what we would expect, namely when $a = 0$ we have that $t = 0$ so the best thing to do for the plant is to absorb all light. In both other cases we have taken a high value for a, namely $a = 10^{18}$ (in $\mathrm{eV/m^2}$ per second). That is, the production of photopigments is costly. In both cases we only had to do a few iterations, since more iterations just gave a result hardly distinguistable from the previous iterations. This suggests that the method used is either very fast in finding the fixed point or convergence is very slow. We discuss this further below.

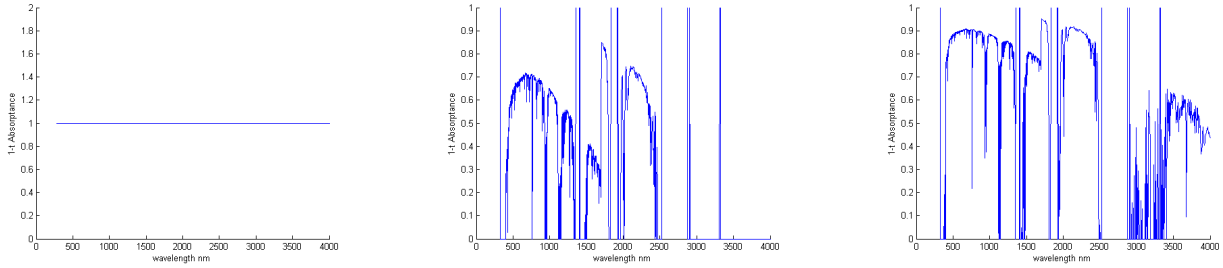

Figure 9: Left: a=0, b=0.5, $t_0 = 0.9 \times \mathbf{1}$. Middle: $a = 10^{18}$, b=0.5, $t_0 = 0.9 \times \mathbf{1}$. Right: $a = 10^{18}$, b=0.01, $t_0 = 0.9 \times \mathbf{1}$. In all cases four iterations have been done.

Figure 10 are the same simulations as before only now we looked at the interval we needed. As mentioned before the visible light is between 400 nm and 700 nm. We looked at a range from 100 nm to 900 nm in this case.

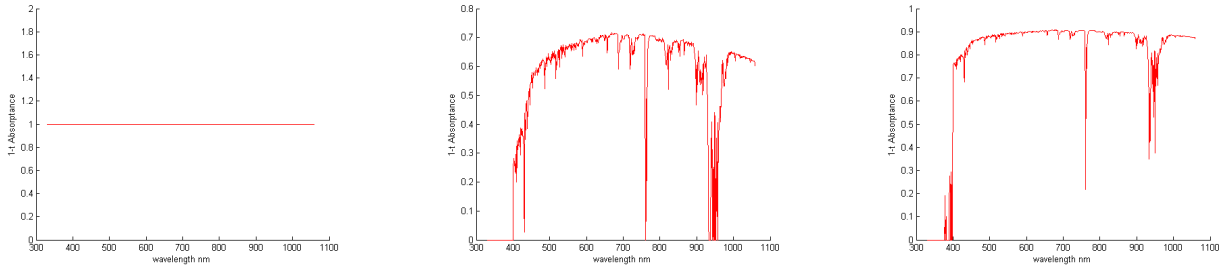

Figure 10: Left: a=0, b=0.5, $t_0 = 0.9 \times \mathbf{1}$. Middle: $a = 10^{18}$, b=0.5, $t_0 = 0.9 \times \mathbf{1}$. Right: $a = 10^{18}$, b=0.01, $t_0 = 0.9 \times \mathbf{1}$. In all cases four iterations have been done.

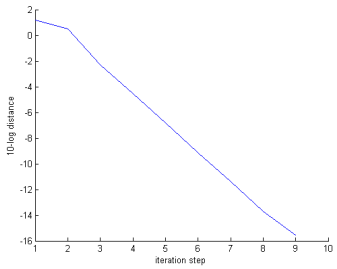

Figure 11: Plot for $\log_{10} ||F(t_k) - t_k||$

In order to investigate the rate of convergence experimentally, we computed for each iteration step k the value $\log_{10} ||F(t_k) - t_k||$. In Figure 11 we plotted the numerical result. It suggests that there is a fast convergence of the iteration process.

5 Discussion

During this project we have tried to follow [1]. In this article it seems that the authors created a model built upon (too) many approximations, which in the 'extreme case' $a = 0, (C_{Pin} = 0)$, no cost, totally fails, while in other cases there are no convincing convergence towards a 'reasonable' solution, see Section 3.4 and 3.5. This triggered us to derive a new master equation. The computation of solutions to this equation using the successive iteration technique seems to give an explanation why the green spectrum could have disappeared from the plants photosystem. This is illustrated in Figure 12.

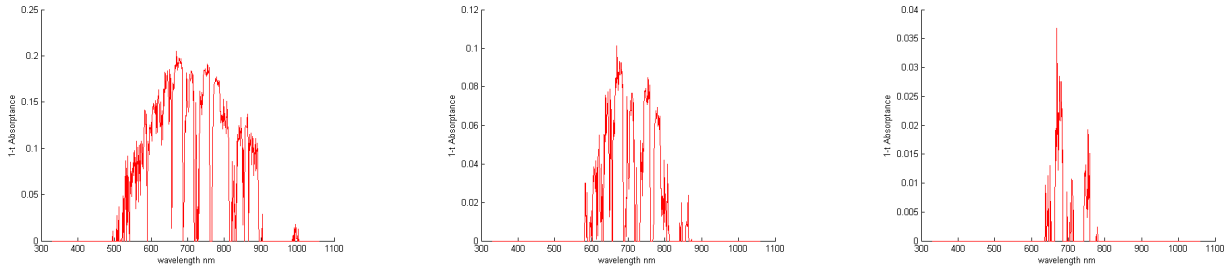

Figure 12: For all $a = 10^{18}$ and $t_0 = 0.9 \times \mathbf{1}$ but $b = 0.8$, $b = 0.82$, $b = 0.83$ from left to right, respectively.

Figure 12 shows that the green light, which is around 555 nm disappears. If we would take $b = 0.84$, then we would get that $t = 1$. This result seems odd as well. We have no explanation of the latter behaviour at this moment.

At the end of this project we still have some open questions:

One question is related to the convergence. The numerical resul on the decrease of the distance $||F(t_k)-t_k||$ shown in Figure 11 is remarkable. The question is, whether one could explain or prove this result analytically.

Another is related to the difference between the original expressions for the excitation frequency for light and darkness. Why should (3) be different from (1)? Is our approach,(33), for J_D not more logical?

Another point we still have open is: how do solutions to the problem depend on the discretization of the (sun)light frequency spectrum? I.e. the choice of cut-off ν_0 and ν_n and the stepsize $\Delta\nu_i$? In the data we used (ASTM) the stepsize started with 0.5 nm, later it became 1.0 nm and in the end the stepsize was even 5.0 nm. We experimented with a different cut off. This did not seem to matter for the result of the iteration procedure.

At this point we would like to remark, that a totally different approach is possible, namely by using (non-linear) optimalisation techniques directly on the explicit form of P_O. This could be a totally new project.

We hope that it will be possible to investigate these questions in the future.

References

[1] Marosvölgyi,M.A. and H.J. van Gorkum (2010), Cost and color of photosynthesis, *Photosynthesis Research* **103**, 105-109.

[2] O. van Gaans, S.C. Hille, R. de Jong, F. Offergeldt, F. Redig, P. Rogaar, F. Ruoff, F. Spieksma, E. van Zwet (2011), 'Onveranderlijkheid geeft grip op een wereld in beweging', *Syllabus LAPP-Top Programma Wiskunde 2011, Mathematisch Instituut, Universiteit Leiden*, 61-73.

[3] Webpage of ASTM concerning sunlight spectrum, http://rredc.nrel.gov/solar/spectra/am1.5/

[4] Ross, R.T. and M.Calvin (1967), Thermodynamics of light emission and free-energy storage in photosynthesis, *Biophysical Journal* **7**, 595-614.

A Main program

```
clear all
clc

n = 2002;
kT = 0.0254; in eV
A = solardata;
h = 4.136e^-15; in eV*s
c = 299.8e6; in m/s
hc = h * c; in eV*m
[Iss_fr, wavelength, energy, IB_fr, freq] = wave_eng(A, h);
I = Iss_fr;
IB = IB_fr;
a = .5;
b = .5;
t = ones(1, 2002) * 0.9;

for i = 1 : 2002
 I_sup(i) = I(i);
  if I(i) == 0
    I_sup(i) = 1.5663e^-041;
  end
end

figure(1)
hold on
xlabel('frequency in THz');
ylabel('I'_0,i);
plot(freq, I_sup);
hold off

for i = 1 : 2002
 IB_sup(i) = IB(i);
  if IB(i) == 0
    IB_sup(i) = 1.5663e^-041;
  end
end

v = I_sup./IB_sup;

figure(2)
hold on;
```

xlabel('frequency in THz');
ylabel('$I_{0,i}/I'_{BB,i}$');
plot(freq,v);
hold off

figure(3)
hold on
xlabel('frequency in THz');
ylabel('$I'_{BB,i}$');
plot(freq, IB_{sup});
hold off

for j = 1 : 2
  [t, l] = iterF(t, kT, a, b, IB_{sup}, I_{sup});
  e(j) = log(l)/log(10);
  t;
end

figure(10);
hold on
plot([1:length(e)],e([1:length(e)]));
hold off

wavekort = wavelength([100 : 900]);
tkort = t([100 : 900]);
figure(4);
clf reset;
hold on;
xlabel('wavelength nm');
ylabel('1 − t Absorptance');
plot(wavekort, 1 − tkort,'r−');
plot(wavelength, 1 − t);
hold off

B From wavelength to frequency representation

function[Iss_{fr}, wavelength, energy, IB_{fr}, freq] = $wave_{eng}$(A, h)

c = 299.8e6; *in m/s*
hc = $6.626e^{-34} * 299.8e6 * 1e9$; *in J*nm*
kT = $4.07e^{-21}$; *in J*

b = zeros(1, 2002);

for i = 0 : 199
 for j = 1 : 10
    b(10 ∗ i + j) = A(i + 1, j);
 end
end
b(1, 2001) = A(201, 1);
b(1, 2002) = A(201, 2);

in nm
wavelength = [linspace(280.0, 400, 241), linspace(401, 1700, 1300), 1702, 1705, linspace(1710, 4000, 459)];

in eV
energy = (4.136 ∗ 299.8)./wavelength;

for i = 1 : 2001
  dellambda(i) = wavelength(i + 1) − wavelength(i);
end
dellambda(2002) = dellambda(2001);

freq=(c./wavelength)/1000;*in Thertz*

Iss = b([1 : 2002]);
Iss_{fr} = (Iss. ∗ wavelength. ∗ dellambda)./hc;

IB_{fr} = (8 ∗ pi ∗ (kT/hc) ∗ c. ∗ dellambda)./(wavelength. ∗ wavelength. ∗ (wavelength + 0.5 ∗ (hc/kT)));

figure(6)
hold on
xlabel('Wavelength(nm)');
ylabel('Spectral irradiance (W/m^{-2}/nm)');
plot(wavelength, Iss);

return

C Iteration

C.1 Original article

function F = iterF(t,kT,a,b,IB,I_{sup})

```
Jl = I_sup. * (1 − t);
Jd = −log(t). * IB;
Sl = sum(Jl);
Sd = sum(Jd);

Fh = (1/(log(Sl/Sd)) + 1) * [(IB./I_sup) * (Sl/Sd) + (a./(kT * I_sup)) * (1/(2 * (1 − sqrt(b))))];

for i = 1 : 2002
  if Fh(i) > 1
    Fh(i) = 1;
  end
end

F = Fh;

return
```

C.2 New iteration

```
function [F,l] = iterF(t,kT,a,b,IB,I_sup)
Jl = I_sup. * (1 − t);
Jd = IB. * (1 − t);
Sl = sum(Jl);
Sd = sum(Jd);
d1 = (I_sup./IB). * (log(1 + (Sl/Sd)) + ((Sl/Sd)/(1 + (Sl/Sd))));
d2 = ((Sl/Sd)^2)/(1 + (Sl/Sd));

F = (a./(kT * IB)). * ((1/(2 * (1 − sqrt(b)))));
Fh = F./(d1 − d2)

for i = 1 : 2002
  if Fh(i) > 1
    Fh(i) = 1;
  end
  if Fh(i) < 0
    Fh(i) = 0;
  end
end

F = Fh;
d = F − t;
l = sqrt(d * d′)
return
```